

## Model for exchange bias in polycrystalline ferromagnet-antiferromagnet bilayers

M. D. Stiles and R. D. McMichael

*National Institute of Standards and Technology, Gaithersburg, Maryland 20899*

(Received 15 April 1998; revised manuscript received 24 August 1998)

This paper describes a model for polycrystalline ferromagnet-antiferromagnet bilayers. Independent antiferromagnetic grains are coupled to a ferromagnetic film both by direct coupling to the net moments at the interfaces of the grains and by spin-flop coupling. Rotation of the ferromagnetic magnetization applies a torque to the antiferromagnetic spins at the interface of each grain which winds up partial domain walls in the antiferromagnet. The model explains both the unidirectional anisotropy that gives rise to the well-known shifted hysteresis loops, and the hysteretic effects observed in rotational torque and ferromagnetic resonance experiments. The unidirectional anisotropy comes from grains in which the antiferromagnetic order is stable as the magnetization is rotated. The hysteretic effects come from grains in which the antiferromagnetic order irreversibly switches as the domain wall is wound up past a postulated critical angle. For all of the models considered here, spin-flop coupling does not contribute to the unidirectional anisotropy.

[S0163-1829(99)01305-3]

### I. INTRODUCTION

The exchange coupling of ferromagnetic and antiferromagnetic films across their common interface significantly modifies some of their properties. The most well-known effect is a shift in the hysteresis loop of the ferromagnet,<sup>1</sup> called exchange bias. In the last ten years there has been considerable interest in exchange-biased ferromagnetic films because the shift can be useful in controlling the magnetization in devices, such as spin valves<sup>2</sup> which sense changing magnetic fields through the giant magnetoresistance effect.<sup>3</sup> Read heads based on this effect are starting to be used in magnetic disk storage.

The loop shift arises when the order in the antiferromagnet is established in the presence of the ferromagnet. By itself, the antiferromagnet can order in any one of its degenerate energy minima. When it is coupled to a ferromagnet, however, it chooses the state that minimizes the energy due to coupling to the ferromagnet. Furthermore, the antiferromagnet is only weakly coupled to external magnetic fields, so it retains a "memory" of the ferromagnetic direction at the time when the antiferromagnetic order was set, even when the ferromagnetic magnetization is later rotated. This coupling is often thought of as a unidirectional anisotropy or as a fixed magnetic field acting at the interface.

The shift in the hysteresis loop is not the only effect that is found in exchange-biased magnetic layers. Several effects, schematically illustrated in Fig. 1, indicate that there are hysteretic processes occurring in these systems as the applied field is varied. Almost all films show an increase in the coercivity when coupled to an antiferromagnet, even when the sample is prepared in a state that does not show a bias. Additionally, in at least some systems, different reversal mechanisms are observed for increasing and decreasing fields.<sup>4-6</sup> This difference means that the average of the two reversal fields is *not* a reliable measure of the size of the unidirectional anisotropy. Since at least one reversal mechanism is likely to be nonuniform, physically meaningful models for the hysteresis loop are likely to be very complicated.

In contrast, experiments done in magnetic fields high

enough to saturate the ferromagnetic magnetization are likely to be easier to model. One such experiment is high field rotational torque,<sup>5,7-9</sup> in which the sample is rotated in a constant field and the torque is measured as a function of angle. The angular variation of the torque can be used to determine the anisotropy of magnetic samples. In exchange-biased films, it is generally found that the torque does not integrate to zero over a full rotation, even in saturating fields. Thus, irreversible work is being done when rotating the magnetization relative to the sample. As shown in Fig. 1(D), the rotational hysteresis remains large in high fields, implying that hysteretic processes play an important role.

Another experiment done in fields high enough to saturate the magnetization is ferromagnetic resonance (FMR), also illustrated in Fig. 1. Since the ferromagnetic resonance condition depends on the curvature of the energy with respect to angular variations of the magnetization direction,<sup>10</sup> FMR can also be used to determine the anisotropy of magnetic samples. Typically, FMR experiments involve a constant frequency excitation and an applied field which is varied to achieve the resonance condition. Anisotropy terms, whether they are intrinsic to the ferromagnet or due to coupling to the antiferromagnet, lead to decreases in the resonance field in the easy directions of the anisotropy and increases in the hard directions. Such variations are observed in FMR experiments on exchange-biased films, but are found to be superimposed on an isotropic negative shift in the resonance field.<sup>11-13</sup> If the uniform shift in the resonance field were only negative for in-plane variation of the magnetization, it could be explained by an increased surface anisotropy. However, since recent measurements<sup>14,15</sup> show that the shift is negative for out-of-plane magnetizations as well, it must arise from hysteretic processes, as discussed in Sec. III B.

Most models for these systems have focused on explaining the size of the loop shift. The simplest model gives a coupling that is orders of magnitude too strong compared to the loop shifts that have been measured.<sup>7</sup> In this model, the unidirectional anisotropy is due to the exchange coupling across an ideal interface between fixed antiferromagnetic spins and the interfacial ferromagnetic spins. The interface is

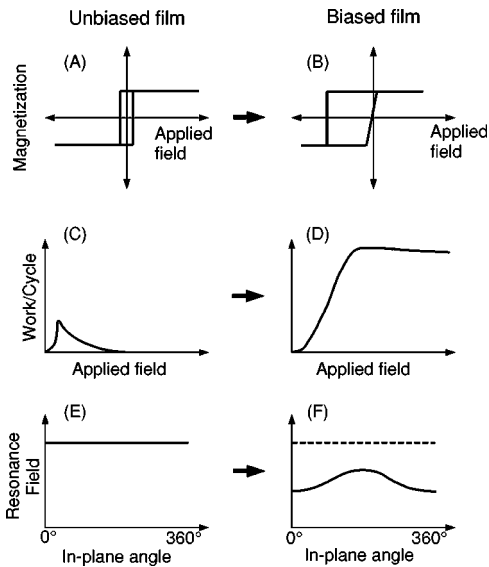


FIG. 1. Experimental characteristics of exchange biasing. Panels (A), (C), and (E) show typical experimental results for free ferromagnetic films. Panels (B), (D), and (F) show how the results change when the film is exchange biased by coupling to an antiferromagnetic film. Compared to panel (A), the magnetization in panel (B) shows a shifted loop, increased coercivity (loop width), and possibly different reversal mechanisms for increasing and decreasing fields. Compared to panel (C), panel (D) shows that energy is dissipated when rotating the sample in an applied field, even at fields high enough to saturate the magnetization. Compared to panel (E) the ferromagnetic resonance field in panel (F) shows an overall shift down, corresponding to an increase in the resonance frequency at fixed field, and angular variation typical of a unidirectional anisotropy.

assumed to be uncompensated, i.e., only one antiferromagnetic sublattice is present. Several effects reduce the loop shift compared to the value predicted by this model. Néel<sup>4</sup> and Mauri *et al.*<sup>16</sup> pointed out that it can be energetically more favorable to form domain walls parallel to the interface in the antiferromagnet than to fix the antiferromagnetic moments and keep the exchange energy at the interface. Allowing the rotation of the magnetization to spread into the antiferromagnet can greatly reduce the expected loop shift.

Néel<sup>4</sup> also pointed out that for realistically rough interfaces, the presence of both antiferromagnetic sublattices at the interface, causing partial compensation of the moments, will lead to a reduction in the coupling and hence the loop shift. For polycrystalline antiferromagnets, the statistical fluctuations in the number of spins at the interface of each grain lead to such partial compensation, i.e., a net moment on each grain. Takano *et al.*<sup>17</sup> have measured a net magnetization in polycrystalline CoO/MgO multilayers, presumably due to uncompensated spins at interfaces. They found the temperature dependence of the net magnetization to be the same as the temperature dependence of the exchange anisotropy in a multilayer in which a similar CoO film is grown next to Ni<sub>80</sub>Fe<sub>20</sub>. This similarity suggests that these uncompensated spins at the interface are important for the exchange anisotropy.

For single-crystal antiferromagnets, rough interfaces lead to vanishing average moments for any macroscopic interface area. Malozemoff<sup>18</sup> showed how domain walls in the system

perpendicular to the interface give rise to coupling for single-crystal systems. In his model, these domain walls can be thought of as effectively breaking the single crystal into a polycrystal.

Koon<sup>19</sup> has shown that spin-flop effects in the antiferromagnet can lead to coupling even for ideal interfaces that are completely compensated, i.e., those with no net moment. Spin-flop coupling favors perpendicular alignment between the ferromagnet magnetization and the sublattice magnetization in the antiferromagnet.

Hysteretic effects, such as the high field rotational hysteresis results and the isotropic FMR field shift, *cannot* be explained by models in which the antiferromagnetic spins are fixed and the ferromagnetic spins are uniform across the layer. In such models, the energy is a single-valued, continuous, and differentiable function of the magnetization direction. In a high field rotational hysteresis experiment with such a well-behaved energy function, the magnetization direction is single valued, closely following the applied field, and no net work is done when the magnetization is returned to its initial direction. Thus there is no high field rotational hysteresis. On the other hand, Néel<sup>4</sup> and Koon<sup>19</sup> showed that rotational hysteresis could result from irreversible motion of domain walls in the antiferromagnet, because the irreversible motion makes the energy function discontinuous. For ferromagnetic resonance, the well-behaved coupling energy would necessarily have regions with positive curvature (easy directions) and negative curvature (hard directions). The isotropic resonance field shift would not be observed because the resonance field would not only go down in directions made easier by coupling, but would also go up in directions made harder.

In this paper, we describe a model that can explain both the unidirectional anisotropy and the hysteretic effects. We consider different limiting cases of a general model in different sections. In Sec. II, we present the model for individual antiferromagnetic grains coupled to a ferromagnetic film. The coupling energy includes the three contributions discussed above, direct coupling to the net moment at the interface of the grain, spin-flop coupling, and partial domain walls in the antiferromagnet. In addition to these energy terms, we include the possibility of instabilities in the antiferromagnet. In Sec. III A, we calculate the unidirectional anisotropy that arises from grains in which the antiferromagnetic order is stable as the ferromagnetic magnetization is rotated. Section III B gives the high field rotational hysteresis and the isotropic FMR field shift that arises from grains in which the order is unstable. In these two sections, III A and III B, we leave out the spin-flop coupling contribution to the energy. In Sec. III C, we discuss the effect of spin-flop coupling on the previous results. We discuss the implications of this model for the coercivity in Sec. IV A, which includes nonuniformities in the ferromagnetic magnetization in the plane of the interface. In Sec. IV B, we discuss the energy scales of domain walls in antiferromagnets. In Sec. IV C, we discuss the reduction of the direct coupling at the interface due to disorder at the interface. In Sec. IV D, we give a simple argument for the existence of spin-flop coupling and a simple estimate of its size. Finally, in Sec. IV E, we discuss the consequences of domain walls in the ferromagnet perpendicular to the interface.

## II. MODEL

In this model, the ferromagnetic layer interacts with independent antiferromagnetic grains. We assume that the applied magnetic field is high enough that the ferromagnetic magnetization can be assumed to be uniform. We also assume that the antiferromagnetic grains are small enough that they do not break up into domains. Each grain is in a single antiferromagnetic state except for any partial domain walls parallel to the interface that are created by the coupling to the ferromagnet. There are three contributions to the energy for each grain coupled to the ferromagnet;

$$\frac{E}{Na^2} = \frac{-J_{\text{net}}}{a^2} [\hat{\mathbf{M}}_{\text{FM}} \cdot \hat{\mathbf{m}}(0)] + \frac{J_{\text{sf}}}{a^2} [\hat{\mathbf{M}}_{\text{FM}} \cdot \hat{\mathbf{m}}(0)]^2 + \frac{\sigma}{2} [1 - \hat{\mathbf{m}}(0) \cdot (\pm \hat{\mathbf{u}})]. \quad (1)$$

For  $N$  spins at the interface of the grain, the interfacial area is  $Na^2$ , where  $a$  is a lattice constant. The important directions are the ferromagnetic magnetization,  $\hat{\mathbf{M}}_{\text{FM}}$ , the direction of the net sublattice magnetization at the interface,  $\hat{\mathbf{m}}(0)$ , and the two easy directions of the uniaxial anisotropy in the antiferromagnet,  $\pm \hat{\mathbf{u}}$ . The energy scales are the average direct coupling to the net moment of the antiferromagnetic grain,  $J_{\text{net}}$ , the spin-flop coupling,  $J_{\text{sf}}$ , and the energy of a  $180^\circ$  domain wall in the antiferromagnet,  $\sigma$ .

The first term in Eq. (1) is the direct coupling at the interface. For each grain the net coupling takes a definite value chosen from a statistical distribution with a mean that is typically smaller than the bare coupling energy  $J_{\text{int}}$  by approximately  $1/\sqrt{N}$ . This is discussed in more detail in Sec. IV C. The second term in Eq. (1) is the spin-flop coupling which favors a perpendicular relative orientation between the magnetizations of the films. The mechanism for this coupling is discussed in more detail in Sec. IV D.

The third term in Eq. (1) is the energy of a partial domain wall in the antiferromagnetic grain wound through an angle determined by  $\cos \alpha^{(\pm)} = \hat{\mathbf{m}}(0) \cdot (\pm \hat{\mathbf{u}})$ . For an individual grain in a thick antiferromagnetic film, all of the spins in the partial domain wall lie in the plane defined by  $\pm \hat{\mathbf{u}}$  and  $\hat{\mathbf{m}}(0)$ . For a given direction of interfacial moment  $\hat{\mathbf{m}}(0)$ , the energy of the partial domain wall in the antiferromagnet depends on the state in which the antiferromagnet is ordered through the sign,  $(\pm)$ . Two partial domain walls are shown in Fig. 2.

For high field rotational hysteresis and the isotropic ferromagnetic resonance field shift to exist, some of the antiferromagnetic grains in the system must make irreversible transitions. To include these transitions in the model, we postulate that some grains have a critical angle  $\alpha_{\text{crit}}$ , such that when the partial domain wall is wound up to an angle greater than  $\alpha_{\text{crit}}$ , the antiferromagnetic order becomes unstable, and the system makes a transition to another state, which has reversed antiferromagnetic order far from the interface. (See Fig. 2 for an example of possible states before and after such a transition.) Then, as the ferromagnetic magnetization is rotated, the partial domain wall is wound up to the critical angle, and a transition occurs.

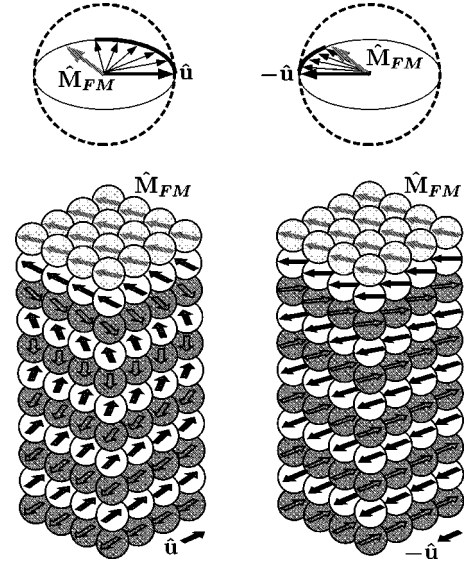


FIG. 2. Two configurations of an antiferromagnetic grain coupled to a ferromagnetic layer. The white spheres are the antiferromagnetic atoms on the sublattice that predominates at the interface, the dark gray spheres are the other sublattice, and the light gray spheres are the ferromagnetic atoms in the bottom atomic layer of the ferromagnetic thin film with a uniform magnetization direction,  $\hat{\mathbf{M}}_{\text{FM}}$ . In each sphere, the arrow gives the direction of the atomic moment. In the structure to the left (right), the antiferromagnet has ordered in the  $\hat{\mathbf{u}}$  ( $-\hat{\mathbf{u}}$ ) direction far from the interface. In each, the coupling with the ferromagnetic layer has wound up a partial domain wall. The directions of the antiferromagnetic spins in one sublattice, and the ferromagnetic spins are given in the top panels.

One mode of instability in antiferromagnetic grains of finite thickness is unwinding from the back surface of the film, the surface opposite the ferromagnet. Néel<sup>4</sup> has extensively studied partial domain walls in antiferromagnetic thin films with in-plane easy axes. Since the back surface of the film is uncoupled, the energy of the partial domain wall as a function of the sublattice magnetization direction at the interface is more complicated than that in Eq. (1). Films thinner than  $\delta/4$  ( $\delta$  is the domain-wall width) only exist in a single state as the interfacial magnetization of the antiferromagnet is rotated, while films thicker than  $\delta/4$  have critical angles that range from  $90^\circ$  to  $180^\circ$  as the thickness of the film approaches infinity.<sup>4</sup> In this thick film limit, the third term in Eq. (1) is a good approximation to the energy until  $\alpha$  is close to the critical angle.

Néel's results hold for ideal films with no additional source of coercivity. Defects in the antiferromagnet may stabilize the antiferromagnetic order, just as they can increase the coercivity of ferromagnetic films. Equally, defects may provide nucleation sites for reversal at smaller critical angles. Additional important nucleation sites for reversal may lie in the grain boundaries. With these unknowns, we allow a more general critical angle and keep the simpler form for the energy, appropriate for an infinitely thick film, than would be implied from Néel's results.

In at least some samples of  $\text{Ni}_{80}\text{Fe}_{20}/\text{NiO}$ , the antiferromagnetic grains have a uniform distribution of crystallographic orientations.<sup>20</sup> While the relationship between the

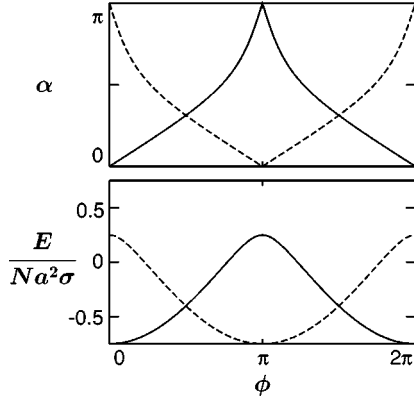


FIG. 3. Domain-wall angle  $\alpha$  and energy of an antiferromagnetic grain coupled to a ferromagnetic layer. For a grain with an easy axis in the  $\hat{x}$  direction and a ratio of coupling strength to domain-wall energy,  $r=1.5$ , the top panel shows, as a function of the angle,  $\phi$  of the ferromagnetic magnetization with respect to the  $x$  axis, the domain-wall angle and the bottom panel shows the energy. In each panel, the solid (dashed) curve gives the result for the sublattice magnetization along  $\hat{u}$  ( $-\hat{u}$ ) far from the interface, see Fig. 2.

propagation direction of the antiferromagnetic order and the easy axes of the antiferromagnetic magnetization can be complicated in thin-film antiferromagnets, we model the system as having a uniform distribution of easy-axis directions. In general, the distribution will not be uniform; when an alternate distribution is measured, it can be averaged over, at least numerically, in a straightforward manner. In addition, there is a distribution of direct coupling strengths. To compare with experiment, all of the results in this paper would need to be averaged over this distribution. At appropriate points, we discuss the effect of this averaging.

### III. RESULTS

#### A. Unidirectional anisotropy

In this section and the next, we ignore the spin-flop coupling. In this case, the energy, Eq. (1), can be readily minimized with respect to the antiferromagnetic magnetization direction at the interface,  $\hat{\mathbf{m}}(0)$ . The minimum is

$$\frac{E^{(\pm)}}{Na^2} = \frac{\sigma}{2} (1 - [1 + 2r\hat{\mathbf{M}}_{\text{FM}} \cdot (\pm\hat{\mathbf{u}}) + r^2]^{1/2}), \quad (2)$$

where  $r = 2J_{\text{net}}/\sigma a^2$ , is the ratio of the direct coupling energy to half a domain-wall energy. The minimum energy configuration has  $\hat{\mathbf{u}}$ ,  $\hat{\mathbf{M}}_{\text{FM}}$ , and  $\hat{\mathbf{m}}(0)$  all lying in a plane. The partial domain wall in the antiferromagnet is wound up through an angle  $\alpha$  defined by

$$\cos \alpha^{(\pm)} = \hat{\mathbf{m}}(0) \cdot (\pm\hat{\mathbf{u}}) = \frac{r\hat{\mathbf{M}}_{\text{FM}} \cdot (\pm\hat{\mathbf{u}}) + 1}{\sqrt{1 + 2r\hat{\mathbf{M}}_{\text{FM}} \cdot (\pm\hat{\mathbf{u}}) + r^2}}. \quad (3)$$

For each direction of the ferromagnetic magnetization, there are two possible states of the system, depending on the state of the antiferromagnet, as specified by the sign,  $(\pm)$ . For one particular grain, the two configurations are illustrated in Fig. 2. Figure 3 shows the energies and angles of domain

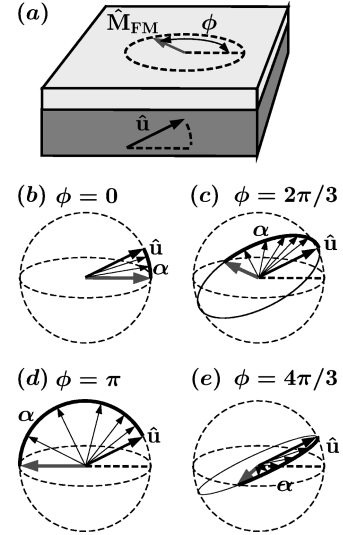


FIG. 4. Unwinding of domain walls. Panel (a) shows the geometry being considered: the ferromagnetic magnetization  $\hat{\mathbf{M}}_{\text{FM}}$  is at an angle  $\phi$  with respect to the  $x$  axis, and the easy axis of the antiferromagnet has a component out of the interface plane, with an in-plane projection along the  $x$  axis. Panels (b)–(e) show the plane of the antiferromagnetic spins in the partial domain-wall as the ferromagnetic magnetization is rotated from the easy direction,  $\phi = 0$ , through the hard direction,  $\phi = \pi$ . Note that the angle of the partial domain wall  $\alpha$  increases when going from the easy direction to the hard direction and then decreases without winding up a complete domain wall.

walls in this grain as a function of the angle of rotation of the ferromagnetic magnetization.

In contrast to the behavior of  $XY$  spins, which we discuss below, Heisenberg spins are not fixed to lie in a particular plane. In fact, the spins in the domain wall are contained in the plane defined by  $\hat{\mathbf{M}}_{\text{FM}}$  and  $\hat{\mathbf{u}}$ , which rotates as the ferromagnetic magnetization is rotated, see Fig. 4. One important consequence of this behavior is that domain walls are never wound up past  $180^\circ$ . The domain wall is wound up to its maximum when the magnetization is opposite the projection of the antiferromagnetic easy axis on the rotation plane. When the magnetization is rotated further, the plane of the domain wall rotates so that the domain wall unwinds rather than winding further. This result is reflected in Eq. (3), where  $\cos \alpha^{(\pm)} < 1$  if  $\hat{\mathbf{M}}_{\text{FM}}$  and  $\hat{\mathbf{u}}$  are not antiparallel. If a complete domain wall were wound up, it would detach from the interface and sweep through the antiferromagnetic grain, erasing the biased state. Thus, this unwinding of domain walls, which occurs for Heisenberg spins, is necessary to preserve the biased state on rotation of the magnetization. This unwinding of the domain wall holds as limiting behavior even when the rotation plane includes the easy axis.

Experimentally, the biased state is prepared by allowing the antiferromagnet to order in the presence of a fixed ferromagnetic magnetization. In the model, we choose the antiferromagnetic state for each grain that gives the lower energy with the ferromagnetic magnetization in the direction in which the biased state is prepared. If the grains have a uniform distribution of orientations, this gives a unidirectional anisotropy with a minimum in the bias direction.

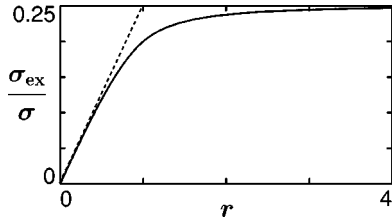


FIG. 5. Unidirectional anisotropy energy for a distribution of stable grains averaged over grain orientations, Eq. (6). The dotted line is  $\sigma_{\text{ex}} = J_{\text{net}}/2a^2$ .

Choosing the lower energy state for each grain corresponds to choosing the sign ( $\pm$ ) in Eq. (2) such that  $\pm \hat{\mathbf{u}} \cdot \hat{\mathbf{M}}_0 > 0$ , where  $\hat{\mathbf{M}}_0$  is the bias direction. Making this choice for the sign and integrating the energy over all orientations of  $\hat{\mathbf{u}}$  amounts to averaging over a half sphere. The result can be expressed in terms of Legendre polynomials of  $\hat{\mathbf{M}}_{\text{FM}} \cdot \hat{\mathbf{M}}_0$

$$\begin{aligned} \frac{E}{A\sigma/2} = & F_0(r) - F_1(r)[\hat{\mathbf{M}}_{\text{FM}} \cdot \hat{\mathbf{M}}_0] \\ & + F_3(r) \frac{1}{2} [5(\hat{\mathbf{M}}_{\text{FM}} \cdot \hat{\mathbf{M}}_0)^3 - 3(\hat{\mathbf{M}}_{\text{FM}} \cdot \hat{\mathbf{M}}_0)] \\ & + \text{higher odd polynomials,} \end{aligned} \quad (4)$$

where  $A$  is the area of the sample (the sum of  $Na^2$  over all grains). The coefficients  $F_n(r)$  of the Legendre polynomials have different forms for  $r < 1$  and  $r > 1$ , but are continuous and twice differentiable at  $r = 1$ ;

$$\begin{aligned} F_0(r) = & \begin{cases} -\frac{r^2}{3} & r < 1, \\ -r + 1 - \frac{1}{3r} & r > 1, \end{cases} \\ F_1(r) = & \begin{cases} \frac{r}{2} \left(1 - \frac{r^2}{5}\right) & r < 1, \\ \frac{1}{2} \left(1 - \frac{1}{5r^2}\right) & r > 1, \end{cases} \\ F_3(r) = & \begin{cases} \frac{r^3}{40} \left(1 - \frac{5r^2}{9}\right) & r < 1, \\ \frac{1}{40r^2} \left(1 - \frac{5}{9r^2}\right) & r > 1. \end{cases} \end{aligned} \quad (5)$$

From this result, the coefficient of the unidirectional anisotropy energy,  $-\sigma_{\text{ex}} \hat{\mathbf{M}}_{\text{FM}} \cdot \hat{\mathbf{M}}_0$  is

$$\sigma_{\text{ex}} = \frac{\sigma}{2} F_1(r), \quad (6)$$

which is plotted in Fig. 5. For weak coupling at the interface compared to the domain-wall energy,  $r < 1$ , the coefficient is approximately  $J_{\text{net}}/2a^2$ . For strong coupling at the interface, it crosses over to approximately  $\sigma/4$ . Averaging this result over a distribution of interface coupling energies broadens

the result somewhat. The behavior is the same in both limits, but the limits are approached more slowly.

## B. Irreversible effects

Both rotational hysteresis and isotropic negative FMR field shifts can be explained by irreversible transitions in antiferromagnetic grains between two states that are degenerate in the absence of coupling to the ferromagnet. In the present model, grains behave in different ways as the ferromagnetic magnetization is rotated in plane, depending on their critical angle  $\alpha_{\text{crit}}$ , their orientation  $\hat{\mathbf{u}}$ , and their ratio  $r$ , of the interfacial coupling energy to domain-wall energy. Grains can either maintain a particular antiferromagnetic order far from the interface (reversible behavior), or they can switch between the two possible states (hysteretic behavior). Reversible grains contribute to the unidirectional anisotropy and hysteretic grains contribute to the rotatable anisotropy seen in FMR and to the high field rotational hysteresis, as explained more fully below. In grains with  $r < 1$ , domain walls are never wound past  $90^\circ$  [see Eq. (3)], so these grains do not switch for  $\alpha_{\text{crit}} > 90^\circ$ . For simplicity, our discussion of instabilities focuses on the case  $\alpha_{\text{crit}} > 90^\circ$ . In grains with  $r > 1$ , domain walls are wound up to  $180^\circ$  when the plane of rotation includes the easy axis of the antiferromagnet. As the easy axis moves further out of the plane toward the rotation axis (here denoted by the interface normal  $\hat{\mathbf{z}}$  for convenience), the winding of the domain wall is less and less affected by motion of  $\hat{\mathbf{M}}_{\text{FM}}$ . Grains with easy axes close enough to the interface normal do not switch when the magnetization is rotated *in-plane* (around  $\hat{\mathbf{z}}$ ). The condition for grains not to switch is determined by comparing the critical angle to the maximum angle through which a domain wall is wound on a full rotation of the ferromagnetic magnetization. Solving this condition for the angle of the easy axis with respect to the interface normal, given by  $\sin \theta = \sqrt{1 - (\hat{\mathbf{u}} \cdot \hat{\mathbf{z}})^2}$ , in terms of the coupling ratio,  $r$  and the critical angle, written in terms of  $w = \cos \alpha_{\text{crit}}$  (note that for  $\alpha_{\text{crit}} > 90^\circ$ ,  $-1 < w < 0$ ), gives

$$\sin \theta < \frac{(1 - w^2) - w \sqrt{r^2 + w^2 - 1}}{r}. \quad (7)$$

These grains which do not switch add a unidirectional anisotropy for in-plane rotation of the ferromagnetic magnetization, but this anisotropy is “erasable” for some out-of-plane rotations of the magnetization. The unidirectional anisotropy contribution of grains which behave reversibly for in-plane rotation of the magnetization is shown in Fig. 6(a) for several values of  $\alpha_{\text{crit}}$ .

Grains with  $r > 1$ , which do not satisfy the condition Eq. (7), switch antiferromagnetic states when the magnetization is rotated in plane (see Fig. 7 for example). Each grain that undergoes hysteretic transitions changes energy by  $\Delta E$  on each transition, where

$$\begin{aligned} \frac{\Delta E}{\sigma Na^2/2} = & + [r^2 + 3 - 2w^2 - 2w \sqrt{r^2 + w^2 - 1}]^{1/2} \\ & - [r^2 - 1 + 2w^2 + 2w \sqrt{r^2 + w^2 - 1}]^{1/2}. \end{aligned} \quad (8)$$

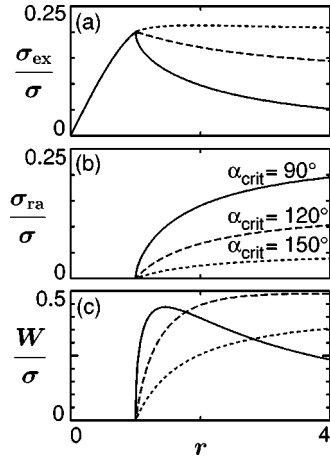


FIG. 6. Hysteretic effects. For three different critical angles,  $90^\circ$  (solid curves),  $120^\circ$  (dashed curves), and  $150^\circ$  (dotted curves), panel (a) gives the unidirectional anisotropy due to grains that, although unstable, are never wound up past the instability point. Panel (b) gives the rotatable anisotropy. Panel (c) gives the work done, due to hysteretic transitions in the antiferromagnetic grains, in one a full rotation of the magnetization in the sample plane. All results have been averaged over the orientations of the grains.

This change in energy is independent of the orientation of the grain, provided the domain wall is wound past its instability point. It is irreversibly lost and dissipated somewhere in the system.

In a high field rotational hysteresis measurement, the work is the angular integral of the torque, which is in turn the angular derivative of the energy. Thus, the work done in a full rotation is equal to the total of the changes in the energy in the irreversible transitions. Each grain that undergoes hysteretic transitions does a total work of  $2\Delta E$  on each full rotation of the magnetization, see Eq. (8). Since the change in energy is independent of the orientation of the grain, averaging over a uniform distribution of grain orientations just gives a factor that is the fraction of grains which undergo irreversible transitions when rotating the magnetization in plane.

Figure 6(c) shows the average work per area per cycle  $W$  for grains with a critical angle  $\alpha_{\text{crit}}$ , a coupling ratio  $r$ , and averaged over easy-axis orientations. In this model, domain walls never get wound past  $90^\circ$ , unless  $r\sin\theta > 1$ , where  $\theta$  is the angle of the easy axis with respect to the interface normal. Thus, as the direct coupling becomes greater than the domain-wall energy,  $r$  increasing past 1, more and more grains undergo irreversible transitions, and the rotational hysteresis increases. As  $r$  increases even further, the energy change in each irreversible transition, Eq. (8), decreases as the direction of the antiferromagnetic magnetization at the interface becomes more and more locked to the ferromagnetic magnetization direction.

The grains that do switch for rotation of  $\hat{\mathbf{M}}_{\text{FM}}$  in a given plane contribute an effective field that tends to be aligned with the current magnetization direction, i.e., a rotatable anisotropy. This effect can be seen in Fig. 7. As the magnetization is rotated in plane, it is on average closer to an energy minimum than to a maximum. The easy direction of that grain switches to stay close to the current direction of the magnetization. With a collection of grain orientations, the

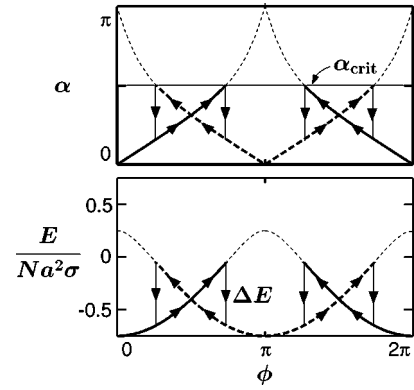


FIG. 7. Energy of a hysteretic antiferromagnetic grain coupled to a ferromagnetic layer. For the grain described in Fig. 3, now with an instability angle  $\alpha_{\text{crit}}$ , the top (bottom) panel shows the domain-wall angle (coupling energy). The thin dotted lines are inaccessible parts of the curves. As the ferromagnetic magnetization is rotated through the angle  $\phi$ , the domain-wall angle eventually exceeds the critical angle, and the antiferromagnetic grain makes a transition to the other state. The transitions are given by the vertical lines, and the energy difference at the critical angle is  $\Delta E$ .

“average” easy direction always stays close to the direction of ferromagnetic magnetization. If we use the critical angle  $\alpha_{\text{crit}}$  to determine which grains switch, but then assume that grains that switch do so as soon as the energy of the other state is lower, the rotatable anisotropy takes the simple form

$$E_{ra} = -\sigma_{ra} \hat{\mathbf{M}}_{\text{FM}} \cdot \hat{\mathbf{M}}_{ra}, \quad (9)$$

where  $\hat{\mathbf{M}}_{ra} = \hat{\mathbf{M}}_{\text{FM}}$ . Note that  $E_{ra}$  is an anisotropy that is constant for all magnetization directions, yet has a nonzero curvature for variations around any direction.<sup>14</sup> Using these assumptions,  $\sigma_{ra}$  is shown in Fig. 6(b). Because grains either contribute to the unidirectional anisotropy or to the rotatable anisotropy, the rotatable anisotropy shown in Fig. 6(b), and the contribution to the unidirectional anisotropy from hysteretic grains shown in Fig. 6(a) add together to give the unidirectional anisotropy for nonhysteretic grains shown in Fig. 5. If the actual reversal is used, the rotatable anisotropy is not exactly aligned with the current direction of the magnetization and depends on the history of the magnetization. However, since the curvature of  $\hat{\mathbf{M}}_{\text{FM}} \cdot \hat{\mathbf{M}}_{ra}$ , which is relevant to FMR measurements, is quadratic in the angular deviation around  $\hat{\mathbf{M}}_{ra} = \hat{\mathbf{M}}_{\text{FM}}$ , the deviation of  $\hat{\mathbf{M}}_{ra}$  from  $\hat{\mathbf{M}}_{\text{FM}}$  does not make a large contribution.

The rotatable anisotropy will make important contributions to other experiments which, like ferromagnetic resonance, are sensitive to the curvature of the free energy around the magnetization direction. Examples of such measurements are Brillouin light scattering,<sup>21</sup> anisotropic magnetoresistance measurements of small-angle perturbations,<sup>22</sup> and ac susceptibility.<sup>23</sup>

Ferromagnetic resonance measurements of the unidirectional anisotropy and the rotatable anisotropy<sup>14,15</sup> show that in at least some samples, the rotatable anisotropy is greater than the unidirectional anisotropy. If the present model applies to these samples, the results shown in Fig. 6 imply both that the direct coupling is large compared to the domain-wall

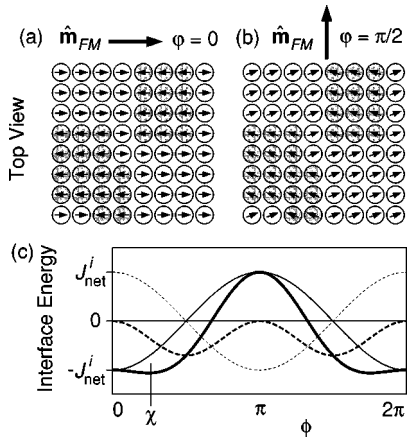


FIG. 8. Antiferromagnetic spins coupled to a ferromagnet. Panels (a) and (b) show a top view of the interfacial spins for the ferromagnetic magnetization in the easy direction of the direct coupling to the antiferromagnet (a) and perpendicular to it (b). In panel (a) the coupling between the ferromagnet and the net moment at the interface of the antiferromagnet is strong and the spin-flop coupling vanishes. In panel (b), the coupling to the net moment vanishes, but spin-flop coupling is substantial. Panel (c) shows the coupling to the net moment (thin solid line), the spin-flop coupling (dashed line), and the total coupling (thick solid line). Also shown is the coupling to the net moment if the antiferromagnet were in the reversed state (dotted line). In this state, the spin-flop coupling is unchanged. The angle  $\chi$  shows the relative angle of minimum energy between the ferromagnetic magnetization,  $\hat{\mathbf{M}}_{\text{FM}}$  and the sublattice magnetization of the antiferromagnet at the interface,  $\hat{\mathbf{m}}(0)$ .

energy and that the critical angle is close to  $90^\circ$  in at least a large fraction of the grains in these samples.

In some systems, it is possible to reduce the interfacial coupling by increasing the width of a spacer layer between the antiferromagnet and the ferromagnet.<sup>24</sup> If all critical angles are greater than  $90^\circ$ , grains with weak interfacial coupling,  $r < 1$ , do not contribute to the hysteretic processes. Once the interfacial coupling is weak enough, the unidirectional anisotropy will decrease proportionally to the average coupling  $\bar{r}$ . In this regime, the rotatable anisotropy and the rotational hysteresis should decrease even faster than the uniaxial anisotropy, roughly as  $1 - \text{erf}(1/\sqrt{\pi\bar{r}})$ .

Schlenker *et al.*<sup>25</sup> have speculated that a “distribution of coercivities in the antiferromagnetic grains” can give reversible and hysteretic behavior. Here, we show that distributions of other properties can also produce these behaviors.

### C. Spin-flop coupling

To investigate the effect of spin-flop coupling, we add it to the model used in the previous section. For completely compensated interfaces with fixed spins, rotating the orientation of the ferromagnetic moment with respect to the antiferromagnetic moments gives rise to no interaction between the films. However, if the moments in the antiferromagnetic sublattices are allowed to cant with respect to each other while the ferromagnetic magnetization is rotated, see Fig. 8, the moments of the antiferromagnet near the interface can tilt a little in the direction of the ferromagnetic moment when

the magnetizations of the two films are perpendicular to each other, lowering the energy of the films and giving rise to the spin-flop coupling.<sup>19</sup>

Figure 8 illustrates how both a direct coupling to the net moment of a grain and the spin-flop coupling coexist in each grain. Like the model in the previous section, the model with spin-flop reduces to simple forms in the limits when the domain-wall energy is either strong or weak compared to the coupling at the interface. In the limit that the domain-wall energy is strong, the energy reduces to the interfacial terms

$$\frac{E}{Na^2} = \frac{J_{\text{net}}}{a^2} [\hat{\mathbf{M}}_{\text{FM}} \cdot (\pm \hat{\mathbf{u}})] + \frac{J_{\text{sf}}}{a^2} (\hat{\mathbf{M}}_{\text{FM}} \cdot \hat{\mathbf{u}})^2. \quad (10)$$

When averaged over orientations, the direct coupling terms give the exchange bias and the spin-flop coupling terms sum to an orientation-independent constant because averaging  $(\hat{\mathbf{M}}_{\text{FM}} \cdot \hat{\mathbf{u}})^2$  (and higher even harmonics) over a half sphere gives an orientation-independent constant. Thus, the spin-flop coupling has no effect on the unidirectional anisotropy in this limit.

However, based on the simple argument given in Sec. IV D, we expect the opposite limit to be relevant. If the spin-flop coupling is stronger than the direct coupling at the interface, we expect that the coupling at the interface is so strong that the moments at the interface will be locked in a configuration that minimizes the interfacial energy, forcing partial domain walls to be wound up in the antiferromagnet. In this limit, the magnetization of the ferromagnet  $\hat{\mathbf{M}}_{\text{FM}}$  and the magnetization of the antiferromagnetic grain at the interface  $\hat{\mathbf{m}}(0)$  are required to make an angle determined by

$$\hat{\mathbf{m}}_{\text{FM}} \cdot \hat{\mathbf{m}}(0) = \cos \chi = \begin{cases} 1 & h < 1 \\ 1/h & h > 1, \end{cases} \quad (11)$$

where  $h = 2J_{\text{sf}}/J_{\text{net}}$ . If the ratio of the couplings is less than one, the two directions are collinear,  $\chi = 0$ .

Locking the spin configuration at the interface requires that partial domain walls be wound up in the antiferromagnetic grains. The minimum energy wall is found when the direction of the antiferromagnetic magnetization at the interface is coplanar with the direction of the ferromagnetic magnetization and the easy axis of the antiferromagnet. In this configuration, the energy of the partial domain wall depends on which state the antiferromagnet is ordered in and is given by

$$\frac{E^{(\pm)}}{Na^2} = \frac{\sigma}{2} (1 - \cos \alpha^{(\pm)}). \quad (12)$$

The energy depends on the angle,  $\alpha^{(\pm)}$  between the antiferromagnetic magnetization at the interface and the easy axis. Using the angles defined above, the domain-wall angles are

$$\alpha^{(-)} = \cos^{-1}[\hat{\mathbf{u}} \cdot \hat{\mathbf{M}}_{\text{FM}}] - \chi, \quad (13)$$

$$\alpha^{(+)} = \pi - \cos^{-1}[\hat{\mathbf{u}} \cdot \hat{\mathbf{M}}_{\text{FM}}] - \chi, \quad (14)$$

and the energy is

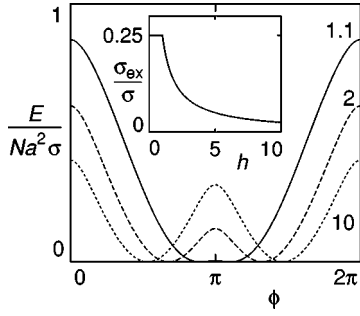


FIG. 9. Variation of coupling energy with the inclusion of spin-flop coupling. The coupling energy, Eq. (15), for a particular antiferromagnetic state for a grain with its easy axis along (1,0,0) is shown for various values of the spin-flop coupling  $h = 2J_{sf}/J_{net}$ ,  $h = 1.1$  (solid),  $h = 2.0$  (dashed),  $h = 10.0$  (dotted). As the spin-flop coupling increases, the unidirectional component decreases and the uniaxial component increases. The inset shows the size of the unidirectional anisotropy energy after averaging over grain orientations, Eq. (16), as a function of the size of the spin-flop coupling.

$$\frac{E^{(\pm)}}{Na^2} = \frac{\sigma}{2} + \frac{\sigma}{2} \left[ \frac{\pm 1}{h} \hat{\mathbf{M}}_{\text{FM}} \cdot \hat{\mathbf{u}} - \frac{\sqrt{h^2 - 1}}{h} \sqrt{1 - (\hat{\mathbf{M}}_{\text{FM}} \cdot \hat{\mathbf{u}})^2} \right]. \quad (15)$$

The first term in the square brackets contributes to the unidirectional anisotropy. The last term in the square brackets in this equation gives the effective spin-flop coupling for this grain. Figure 9 shows energy for a typical grain in one antiferromagnetic state as the magnetization is rotated in plane, for several ratios of spin-flop coupling to direct coupling. For spin-flop coupling weaker than the direct coupling,  $h < 1$ ,  $h$  should be replaced by 1 in Eq. (15). In this limit the spin-flop coupling has no effect whatsoever.

Figure 9 shows how the energy varies as a function of the rotation angle of the ferromagnetic magnetization as the spin-flop coupling is increased. When the spin-flop coupling is comparable to the direct coupling,  $h \geq 1$ , the energy for this grain has a strong unidirectional component. As the spin-flop coupling increases, the unidirectional component decreases and the uniaxial component increases. In the limit of pure spin-flop coupling,  $h \rightarrow \infty$ , there is no unidirectional component at all.

When the energy, Eq. (15), is averaged over the easy-axis orientations, the result in the biased state is

$$\frac{E}{A} = -\frac{\sigma}{4h} \hat{\mathbf{M}}_{\text{FM}} \cdot \hat{\mathbf{M}}_0. \quad (16)$$

Note that the effective spin-flop parts of the interaction in Eq. (15) make no contribution to the total interaction, Eq. (16), as was the case in the limit of large domain-wall energy. What remains is the same as found without spin flop but has the additional factor of  $1/h$ , provided  $h > 1$ . The unidirectional anisotropy constant is shown in the inset of Fig. 9. In the limit of strong spin-flop coupling, the unidirectional anisotropy goes to zero like  $1/h = J_{net}/2J_{sf}$  because domain walls never get wound up past  $90^\circ$ . In Sec. III A, we discussed how domain walls in Heisenberg antiferromagnets with uniaxial anisotropy never get wound up past  $180^\circ$  with direct coupling. Similarly,  $90^\circ$  partial domain walls can unwind with spin-flop coupling at the interface. Equations (13)

and (14) show that in the limit of strong spin-flop coupling, where  $\chi \rightarrow \pi/2$ , the domain-wall angles satisfy  $|\alpha^{(\pm)}| \leq \pi/2$ , since the range of  $\cos^{-1}[\hat{\mathbf{u}} \cdot \hat{\mathbf{M}}_{\text{FM}}]$  is 0 to  $\pi$ .

Thus, the inclusion of spin-flop coupling reduces the unidirectional anisotropy dramatically. If we assume that the spin-flop energy  $J_{sf}$  is one third of  $J_{int}$  as found by Koon,<sup>19</sup> and 30 nm is a typical grain diameter, then, the number of interface spins is roughly  $N \approx 10\,000$ , and the value of  $h$  is approximately 75. When divided by this factor, typical domain-wall energies, see Sec. IV B become too small to give the observed bias. Either the simple estimates for the size of the spin-flop coupling are grossly in error or there are other assumptions of the model that lead to incorrect behavior.

One way to change the model so that it will stabilize domain walls wound past  $90^\circ$  with spin-flop coupling is to change the anisotropy of the antiferromagnet. If the dominant anisotropy is an easy-plane, rather than an easy-axis anisotropy, and there is a smaller easy-axis anisotropy in the easy-plane, the system can be modeled by a collection of XY spins with uniaxial anisotropy. This is the model originally studied by Koon.<sup>19</sup> In this model, the domain wall cannot unwind by changing its plane of rotation because the spins in the domain wall are forced to lie in a particular plane. This allows domain walls to be wound past  $90^\circ$  and hence to give rise to a unidirectional anisotropy. However, when a domain wall is wound up to  $180^\circ$ , it still cannot unwind, and in the absence of any other source of coercivity in the antiferromagnet, the domain wall can detach from the interface and propagate through the antiferromagnet, erasing the biased state.

Looking at the model with XY spins in more detail, the energy, Eq. (1) does not change, except that the antiferromagnetic magnetization is constrained to be perpendicular to some direction,  $\hat{\mathbf{p}}$ . The first consequence of this is that even in the limit in which the interfacial coupling is strong compared to the domain-wall energy, the interfacial coupling cannot necessarily take its minimum value because the antiferromagnetic spins cannot rotate out of their allowed plane. With this constraint, in the limit of strong interfacial coupling, the domain-wall angles, Eqs. (13) and (14), become

$$\alpha^{(-)} = \cos^{-1} \left[ \frac{\hat{\mathbf{u}} \cdot \hat{\mathbf{M}}_{\text{FM}}}{\sqrt{1 - (\hat{\mathbf{p}} \cdot \hat{\mathbf{M}}_{\text{FM}})^2}} \right] \pm \cos^{-1} \left[ \frac{1}{h} \frac{1}{\sqrt{1 - (\hat{\mathbf{p}} \cdot \hat{\mathbf{M}}_{\text{FM}})^2}} \right], \quad (17)$$

$$\alpha^{(+)} = \pi - \cos^{-1} \left[ \frac{\hat{\mathbf{u}} \cdot \hat{\mathbf{M}}_{\text{FM}}}{\sqrt{1 - (\hat{\mathbf{p}} \cdot \hat{\mathbf{M}}_{\text{FM}})^2}} \right] \pm \cos^{-1} \left[ \frac{1}{h} \frac{1}{\sqrt{1 - (\hat{\mathbf{p}} \cdot \hat{\mathbf{M}}_{\text{FM}})^2}} \right], \quad (18)$$

where  $\hat{\mathbf{u}}$  is the anisotropy axis perpendicular to  $\hat{\mathbf{p}}$ . When the absolute value of the argument of the last  $\cos^{-1}$  in each equation is greater than one, the argument should be replaced by one, setting the terms to zero.



An important difference between the model with Heisenberg spins and this model with  $XY$  spins, is that the argument of the first  $\cos^{-1}$  in Eqs. (17),(18) has the extreme values  $\pm 1$  when  $\hat{\mathbf{M}}_{\text{FM}}$  is rotated through  $360^\circ$  (in any plane). In this case, rotating the ferromagnetic magnetization winds up complete domain walls, in contrast to the case of the model with Heisenberg spins, in which the partial domain walls unwind, as discussed in Sec. III A. The complete domain walls are not attached to the interface as the partial domain walls are. When the complete domain wall detaches from the interface and sweeps through the grain, it essentially switches the antiferromagnetic order far from the interface. The partial domain wall then makes a transition from  $\alpha^{(\pm)} = \pm \pi$  to  $\alpha^{(\mp)} = 0$ . After the transitions, the energy in the partial domain wall can be described either as going to zero, with a domain-wall energy irreversibly lost, or as continuing to increase above a domain-wall energy.

An alternate possibility to switching the antiferromagnetic order is that the complete domain walls get pinned somewhere in the antiferromagnet by some additional source of coercivity, allowing multiple domain walls to be wound up. Either of these possibilities have experimental consequences that should be observable in rotational torque experiments. If the domain walls propagate out the back of the sample, the bias would be partially “erased” in experiments in which the (saturated) magnetization is rotated through some large angle. Such behavior is not seen in ferromagnetic resonance experiments.<sup>14</sup> On the other hand, winding of multiple walls should also be observable in a rotational torque experiment in which the magnetization is rotated a full circle in one direction, and then rotated back in the opposite direction. The rotational hysteresis should be significantly less on the return trip than it was on the forward trip since the antiferromagnetic domain walls will contribute a restoring torque.

## IV. DISCUSSION

### A. Coercivity

Predicting the coercivity from the model described above is more complicated than predictions for experiments in which the ferromagnetic magnetization is uniform. Since the coercivity of a biased film is generally quite different than the coercivity of a similar, but unbiased film, it is not correct to use the same model of magnetization reversal that describes the unbiased film. If the reversal mechanism are different for increasing and decreasing magnetic fields,<sup>6</sup> two models for the coercivity would be needed.

In one qualitative model for a hysteresis measurement, as the field is reduced from saturation, the antiferromagnetic grains apply torques to the ferromagnetic magnetization that vary from grain to grain in magnitude, and direction. This variation in torques leads to ripple in the ferromagnetic magnetization in the plane of the interface. With the field applied parallel or antiparallel to the bias direction, there are torques in both directions, so that some parts of the system will nucleate clockwise reversal while others will nucleate counterclockwise reversal. These variations lead to a barrier for reversal, and lead to irreversible work being done in the ferromagnet when that barrier is overcome. However, for applied fields perpendicular to the bias direction (but still in the interface plane), all of the local torques are in the same di-

rection so the barrier to reversal is significantly reduced. This reduction in the coercivity for perpendicular field directions has been observed experimentally.<sup>26</sup>

Even for perpendicular field directions, coupling to the antiferromagnetic grains should still increase the coercivity, due to hysteretic behavior in the antiferromagnetic grains. If the width of domain walls in the ferromagnet is much larger than the grain size, the magnetization reversal effectively proceeds by local coherent rotation, from the perspective of the antiferromagnetic grains. If this rotation had the same sense for increasing and decreasing fields, the hysteretic transitions would contribute an area to the hysteresis loop equal to the high field rotational hysteresis. However, it is likely that the rotation will be in opposite senses for increasing and decreasing fields. This means that there will be parts of the system that behave irreversibly in the rotational hysteresis measurement, but not in magnetization reversal. Thus we expect that the contribution to the area of the hysteresis loop from these hysteretic transitions will be somewhat smaller than the high field rotational hysteresis. On the other hand, there are likely to be some irreversible processes intrinsic to the ferromagnet associated with nonuniform domain-wall motion in the ferromagnet. These processes will increase the area of the hysteresis loop, but will not affect the high-field rotational hysteresis measurement.

Other models have been developed to describe the thermal and temporal behavior of exchange-bias systems. Néel<sup>4</sup> developed an analogy between the behavior of an antiferromagnet and a standard phenomenological model for a ferromagnet. From this analogy, he provides explanations for the behavior of exchange-bias systems when the hysteresis loop is cycled through several times. Fulcomer and Charap<sup>27</sup> developed a model for the thermal behavior by considering a distribution of antiferromagnetic grains with simple behavior. The thermal instability of the grains gives rise to the temperature dependence of the exchange bias.<sup>27-29</sup>

The model presented here differs from that given by Fulcomer and Charap<sup>27</sup> in several respects. In that model, the antiferromagnetic grains have a uniform orientation and a uniform magnetization. They have distributions of interfacial coupling energies and barriers to reversal. In the present model, the antiferromagnetic grains have completely random orientations and partial domains walls. We consider the effects of instability in the grains on measurements like ferromagnetic resonance and rotational torque. However, we have not considered detailed distributions of critical angles or associated energy barriers.

### B. Antiferromagnetic domain walls

The properties of domain walls in the antiferromagnet are determined by the antiferromagnet's exchange coefficient  $A_{\text{AF}}$ , and anisotropy energies  $K_{\text{u}}$ ; for uniaxial anisotropy, the domain-wall energy is  $\sigma = 4\sqrt{A_{\text{AF}}K_{\text{u}}}$ , and the domain-wall width is  $\delta = \pi\sqrt{A_{\text{AF}}/K_{\text{u}}}$ . The exchange coefficient,  $A_{\text{AF}}$ , is related to the exchange constant,  $J_{\text{AF}}$  by  $A_{\text{AF}} = fJ_{\text{AF}}S_{\text{AF}}^2/a$ , where  $f$  is a numerical factor of order unity that depends on the crystal structure,  $a$  is a lattice constant, and  $S_{\text{AF}}$  is the length of the spin. When the thickness of the antiferromagnet is small enough compared to a domain-wall width, a partial domain wall will “see” the end of the film and unwind itself, switching the antiferromagnetic spins far

from the interface, and removing the bias effect.<sup>4</sup> Experiments<sup>9,30,31</sup> show that the exchange bias does not set in for NiO until the thickness is about 40 nm. This thickness can be used as an estimate of the domain wall width in these thin films.

There are several experiments that have yielded values of  $A_{AF}$  and  $K_u$ , for bulk and single-crystal antiferromagnets.<sup>32,33</sup> In bulk NiO, the strongest anisotropy is an easy-plane anisotropy; the domain-wall properties for rotations of the spins out of this plane are  $\sigma_{AF} \approx 12.4$  mJ/m<sup>2</sup> and  $\delta_{AF} \approx 11$  nm.<sup>32</sup> In this easy plane, there is a weaker sixfold anisotropy; the domain-wall properties for rotations of the spin in the easy plane are,  $\sigma_{AF} \approx 0.068$  mJ/m<sup>2</sup>, and  $\delta_{AF} \approx 2.0$   $\mu$ m.<sup>33</sup> In bulk FeF<sub>2</sub>, the dominant anisotropy is uniaxial; the properties of the domain wall are  $\sigma_{AF} \approx 6.4$  mJ/m<sup>2</sup>, and  $\delta_{AF} \approx 1.38$  nm. These values may be useful as a guide for evaluating theoretical results, but there is convincing evidence that the anisotropy of some antiferromagnetic materials is different in thin films, perhaps because of stresses in the films. In CoO/Fe<sub>3</sub>O<sub>4</sub> [001] multilayers, for example, the Co spins lie along the  $[1\bar{1}0]$  or  $[110]$  directions,<sup>34</sup> while in bulk CoO, the spins have three easy axes canted 8° out of each 111 plane.<sup>35</sup> Also, in single-crystal platelets of NiO, the surface can be ‘‘lightly pressed’’ to orient the alternating planes of spins.<sup>33</sup>

### C. Direct interfacial coupling

At the interface between the ferromagnet and the antiferromagnet, there are two contributions to the coupling energy, direct collinear coupling to the net moment of the antiferromagnet and indirect spin-flop coupling. In this section and the next, we present simple estimates of the size of both. The strength of the direct coupling depends on the degree of compensation of the moments at the interface and on the interfacial area of the independent parts of the antiferromagnet. A completely compensated interface has the same number of moments from each magnetic sublattice of the antiferromagnet, and hence no net moment. However, over finite areas the compensation is not exact because the interfaces are rough. In particular, the interface of each grain in a polycrystalline antiferromagnet will have a small net moment, due to a predominance of spins from one sublattice or the other at the interface. Even nominally uncompensated interface orientations, those on which moments from one sublattice predominate for ideal interfaces, will be mostly compensated due to the roughness at the interface exposing terraces of both sublattices. Because of the roughness of the interfaces, we assume that each grain of an antiferromagnet has an almost compensated magnetic interface, regardless of the crystallographic orientation.

If the difference in the number of spins from the two sublattices is statistically distributed around zero, the mean magnitude of the difference is proportional to  $\sqrt{N}$ , for a grain with  $N$  spins at the interface.<sup>17</sup> The total direct exchange coupling between the ferromagnet, assumed to be uniform, and this grain is then equal to the exchange constant  $J_{int}$  for an individual pair of spins across the interface times the net number of spins. Thus the average magnitude per spin of the direct coupling is roughly  $J_{net} \approx J_{int}/\sqrt{N}$ . The interfacial exchange constant,  $J_{int}$ , is usually assumed to be

similar in magnitude to the exchange constant in the ferromagnet or the antiferromagnet. Typical exchange constants are  $J_{AF} \approx 19$  meV in NiO (Ref. 32) and about  $J_{FM} \approx 10$ – $50$  meV in fcc alloys of Ni and Fe.<sup>36</sup> However, we note that, since the exchange mechanism in the ferromagnet is direct and the exchange mechanism in the antiferromagnet may be superexchange for example, as in NiO, the interfacial exchange constant may be very different from either of the bulk values.

### D. Spin-flop coupling

The strength of the spin-flop coupling depends on the interfacial exchange  $J_{int}$  and an effective exchange  $J_{eff}$ , which is related to the antiferromagnetic exchange  $J_{AF}$  by a simple numerical factor. To estimate the strength of the spin-flop coupling consider the situation when the ferromagnet spins and the antiferromagnetic spins are essentially perpendicular to each other. Then, if the antiferromagnetic spins cant at a small angle  $\delta\theta$ , the interfacial energy per antiferromagnetic spin is reduced by approximately  $J_{int}n_{int}\delta\theta$ , where  $n_{int}$  is the number of nearest-neighbor ferromagnetic spins coupled to each antiferromagnetic spin at the interface. At the same time, the antiferromagnet energy is increased by approximately  $J_{AF}(n_{AF}/2)(2\delta\theta)^2/2$ , where  $n_{AF}$  is the number of nearest-neighbor spins of the opposite sublattice for an antiferromagnetic spin at the interface. There are additional contributions for neighbors below the interface, which can be included by making  $n_{AF}$  an effective number of neighbors. Because the interfacial energy reduction is linear in  $\delta\theta$  and the antiferromagnet energy increase is quadratic, there is a minimum in the combined energy,  $-J_{int}^2n_{int}^2/(4J_{AF}n_{AF})$ . Since  $n_{int}$  and  $n_{AF}$  depend on the interface geometry, we characterize the spin-flop coupling by an effective exchange interaction,  $J_{sf} = J_{int}^2/J_{eff}$ . For each grain, the total spin-flop coupling is given by this energy times the number of interfacial spins  $N$  for that grain.

For typical grain sizes and for comparable values of the interfacial exchange constant and the antiferromagnetic exchange constant, this simple argument implies that the spin-flop coupling is much stronger than the direct coupling to the net moment of each grain. The average magnitude of the net direct coupling is reduced from the exchange constant  $J_{int}$  by a factor of  $\sqrt{N}$ , but the spin-flop coupling is only reduced from  $J_{int}$  by the factor  $J_{int}/J_{eff}$ . There is experimental evidence in several systems<sup>34,37</sup> that the antiferromagnetic moments are perpendicular to the ferromagnetic moments.

### E. Ferromagnetic domain walls

In this section, we focus on domain walls in the ferromagnet *parallel* to the interface. In a soft ferromagnet, the properties of domain walls are mainly determined by the applied field and the exchange, when the applied field is higher than the anisotropy fields of the ferromagnet. In this case, the domain-wall energy,  $8\sqrt{2}\mu_0HM_{FM}A_{FM}$ , increases and the domain-wall width,  $4\pi\sqrt{A_{FM}/2\mu_0HM_{FM}}$ , decreases with the square root of the applied field,  $H$ . Here  $M_{FM}$  is the magnetization of the ferromagnet, and  $A_{FM}$  is the exchange coefficient. Thus, for high enough applied field, the domain-wall will be completely squeezed out of the ferromagnet and into the antiferromagnet. The size of the necessary field is set by the domain-wall energy of the antiferromagnet.

If the hysteretic processes that contribute to the isotropic FMR field shift and the high field rotational hysteresis occur in the ferromagnet, the field dependence of these effects should be different than if they occur only in the antiferromagnet. In the ferromagnet, the winding of domain walls parallel to the interface could give an isotropic FMR field shift and a high field rotational hysteresis if the ferromagnet makes irreversible transitions between configurations. However, if such irreversible processes do not occur in the antiferromagnet, both effects should go away in fields high enough to push domain walls into the antiferromagnet. In addition, when there are partial domain walls in the ferromagnet, the ferromagnetic magnetization is not fully saturated. In many exchange-biased systems, the remanent magnetization is very close to the saturation magnetization, implying that domain walls cannot occupy a large fraction of the film thickness. In an  $\text{Ni}_{81}\text{Fe}_{19}/\text{FeMn}$  exchange-bias system, neutron-scattering measurements<sup>38</sup> showed that there was no domain wall in the ferromagnetic  $\text{Ni}_{81}\text{Fe}_{19}$ . While there are indications that domain walls parallel to the interface in the ferromagnet could be important in other systems,<sup>34,22</sup> we assume that the applied field is large enough to saturate the ferromagnetic magnetization.

## V. SUMMARY

The results in this paper fall into two basic categories. In Sec. II, we presented a model to explain both unidirectional anisotropy (Sec. III A) and hysteretic effects (III B) that are seen experimentally in exchange-bias systems. Then in Sec. III C, we discussed the behavior of different models for the interfacial coupling and the symmetry of the antiferromagnetic spins.

The rotational hysteresis seen in high field rotational torque measurements and the isotropic resonance field shift seen in ferromagnetic resonance measurements both suggest that there are irreversible processes occurring in at least some multilayers that exhibit an exchange bias. Since these measurements are done in magnetic fields high enough to saturate the ferromagnetic magnetization, these irreversible processes must occur in the antiferromagnet. Irreversible processes in the antiferromagnet imply that the exchange bias is more complicated than simply a coupling to a fixed antiferromagnetic state. In fact, these irreversible processes imply that the coupling must be strong enough in some antiferromagnetic grains to reverse the order far from the interface.

The loop shift seen in hysteresis measurements as well as the high field rotational hysteresis and the isotropic FMR field shift can be explained by a model in which the ferromagnet is coupled to independent antiferromagnetic grains with random orientations. Here, we have assumed that the antiferromagnet consists of Heisenberg spins with uniaxial anisotropy and that the coupling at the interface is the direct coupling of the ferromagnetic magnetization to the net predominance of one antiferromagnetic sublattice over the other at the grain interface. The exchange bias comes about because the antiferromagnetic order is established in the presence of the ferromagnetic magnetization, and the strength of the bias is approximately set by the lesser of the strength of the average direct coupling and the domain-wall energy.

To explain the irreversible processes, we postulate that in

TABLE I. Unidirectional anisotropy for several models. For different limiting cases of the relative values of the domain-wall energy  $\sigma$ , the direct coupling at the interface  $J_{\text{net}}$ , and the spin-flop coupling  $J_{\text{sf}}$ , this table gives the bounds on the angles of partial domain walls  $\alpha$ , and the size of the unidirectional anisotropy  $\sigma_{\text{ex}}$ . “No bound” implies that (multiple) domain walls can be wound up past  $180^\circ$ , which then makes the exchange bias “erasable.”

Energy limits		Heisenberg spins		XY spins	
		$\alpha$	$\sigma_{\text{ex}}$	$\alpha$	$\sigma_{\text{ex}}$
$\sigma \gg J_{\text{net}}$	$J_{\text{sf}}=0$	$\approx 0$	$J_{\text{net}}/2a^2$	$\approx 0$	$J_{\text{net}}/2a^2$
$\sigma \gg J_{\text{sf}}$	$J_{\text{net}}=0$	$\approx 0$	0	$\approx 0$	0
$J_{\text{net}} \gg \sigma$	$J_{\text{sf}}=0$	$\leq 180^\circ$	$\sigma/4$	No bound	Erasable
$J_{\text{sf}} \gg \sigma$	$J_{\text{net}}=0$	$\leq 90^\circ$	0	No bound	Erasable

some grains the coupling at the interface is strong enough to wind up partial domain walls in the antiferromagnet as the ferromagnetic magnetization is rotated. The state of these grains becomes unstable if the partial domain walls are wound past some critical angle. When the domain walls are wound past this angle, the antiferromagnetic order in the grain changes irreversibly. As the magnetization is rotated in the plane, the energy lost in these transitions gives the hysteresis seen in rotational torque experiments. In addition, the transitions in the unstable grains put the system in lower energy states; this means that on average the easy direction of these grains points toward the ferromagnetic magnetization. This behavior can be described as a rotatable anisotropy, always favoring the present magnetization direction. The rotatable anisotropy gives rise to an isotropic FMR field shift.

Table I summarizes the results of the models considered in this paper. For both Heisenberg spins and XY spins, if the total interfacial coupling is not strong enough to wind up domain walls in the antiferromagnet, the direct coupling gives a unidirectional anisotropy and the spin-flop coupling contributes a uniaxial anisotropy (from each grain), but no unidirectional anisotropy. For Heisenberg spins, if the total interfacial coupling is strong enough to wind up partial domain walls, the direct coupling gives a unidirectional anisotropy which is reduced by the spin-flop coupling because the partial domain walls tend to unwind when they get wound up close to  $90^\circ$ . In the limit that the spin-flop coupling is much stronger than the direct coupling, the unidirectional component goes to zero. For XY spins and strong interfacial coupling, direct coupling and spin-flop coupling behave similarly. When the coupling is strong enough to wind up partial domain walls in the antiferromagnet, the walls do not unwind, but rather complete domain walls get wound up. These are pushed away from the interface, and propagate out the back surface of the antiferromagnet, effectively reversing the antiferromagnetic state.

## ACKNOWLEDGMENTS

This work was supported in part (R.D.M.) by the NIST Advanced Technology Program. The authors would like to thank J. A. Borchers, R. J. Celotta, A. Davies, Y. Ijiri, and D. T. Pierce for critical readings of the manuscript.

- <sup>1</sup>W. H. Meiklejohn and C. P. Bean, *Phys. Rev.* **102**, 1413 (1956).
- <sup>2</sup>B. Dieny, V. S. Speriosu, S. Metin, S. S. P. Parkin, B. A. Gurney, P. Baumgart, and D. R. Wilhoit, *J. Appl. Phys.* **69**, 4774 (1991).
- <sup>3</sup>M. N. Baibich, J. M. Broto, A. Fert, F. Nguyen Van Dau, F. Petroff, P. Etienne, G. Creuzet, A. Friederich, and J. Chazelas, *Phys. Rev. Lett.* **61**, 2472 (1988); G. Binasch, P. Grünberg, F. Saurenbach, and W. Zinn, *Phys. Rev. B* **39**, 4828 (1989).
- <sup>4</sup>L. Néel, *Ann. Phys. (Paris)* **2**, 61 (1967); an English translation is available, in *Selected Works of Louis Néel*, edited by N. Kurti (Gordon and Breach, New York, 1988), p. 469.
- <sup>5</sup>D. Paccard, C. Schlenker, O. Massenet, R. Montmory, and A. Yelon, *Phys. Status Solidi* **16**, 301 (1966).
- <sup>6</sup>V. I. Nikitenko, V. S. Gornakov, L. M. Dedukh, Yu. P. Kabanov, A. F. Khapitov, A. J. Shapiro, R. D. Shull, A. Chaiken, and R. P. Michel, *Phys. Rev. B* **57**, R8111 (1998).
- <sup>7</sup>W. H. Meiklejohn, *J. Appl. Phys.* **33**, 1328 (1962).
- <sup>8</sup>C. Schlenker, *J. Phys. (Paris), Colloq.* **29**, C2-157 (1968).
- <sup>9</sup>C.-H. Lai, H. Matsuyama, R. L. White, T. C. Anthony, and G. G. Bush, *J. Appl. Phys.* **79**, 6389 (1996).
- <sup>10</sup>J. Smit and H. G. Beljers, *Philips Res. Rep.* **10**, 113 (1955).
- <sup>11</sup>V. S. Speriosu, S. S. P. Parkin, and C. H. Wilts, *IEEE Trans. Magn.* **23**, 2999 (1987).
- <sup>12</sup>W. Stoecklein, S. S. P. Parkin, and J. C. Scott, *Phys. Rev. B* **38**, 6847 (1988).
- <sup>13</sup>R. D. McMichael, W. F. Egelhoff, Jr., and L. H. Bennett, *IEEE Trans. Magn.* **31**, 3930 (1995).
- <sup>14</sup>R. D. McMichael, M. D. Stiles, P. J. Chen, and W. F. Egelhoff, Jr., *J. Appl. Phys.* **83**, 7037 (1998); R. D. McMichael, M. D. Stiles, P. J. Chen, and W. F. Egelhoff, Jr., *Phys. Rev. B* **58**, 8605 (1998).
- <sup>15</sup>P. Lubitz, J. J. Krebs, M. M. Miller, and S. Cheng, *J. Appl. Phys.* **83**, 6819 (1998).
- <sup>16</sup>D. Mauri, H. C. Siegmann, P. S. Bagus, and E. Kay, *J. Appl. Phys.* **62**, 3047 (1987).
- <sup>17</sup>K. Takano, R. H. Kodama, A. E. Berkowitz, W. Cao, and G. Thomas, *Phys. Rev. Lett.* **79**, 1130 (1997).
- <sup>18</sup>A. P. Malozemoff, *Phys. Rev. B* **35**, 3679 (1987); *J. Appl. Phys.* **63**, 3874 (1988).
- <sup>19</sup>N. C. Koon, *Phys. Rev. Lett.* **78**, 4865 (1997).
- <sup>20</sup>W. F. Egelhoff, Jr. (unpublished).
- <sup>21</sup>A. Ercole, T. Fujimoto, M. Patel, C. Daboo, R. J. Hicken, and J. A. C. Bland, *J. Magn. Magn. Mater.* **156**, 121 (1996).
- <sup>22</sup>B. H. Miller and E. D. Dahlberg, *Appl. Phys. Lett.* **69**, 3932 (1996).
- <sup>23</sup>V. Ström, B. J. Jönsson, K. V. Rao, and E. D. Dahlberg, *J. Appl. Phys.* **81**, 5003 (1997).
- <sup>24</sup>N. J. Gökemeijer, T. Ambrose, and C. L. Chien, *Phys. Rev. Lett.* **79**, 4270 (1997).
- <sup>25</sup>C. Schlenker, S. S. P. Parkin, J. C. Scott, and K. Howard, *J. Magn. Magn. Mater.* **54-57**, 801 (1986).
- <sup>26</sup>T. Ambrose, R. L. Sommer, and C. L. Chien, *Phys. Rev. B* **56**, 83 (1997).
- <sup>27</sup>E. Fulcomer and S. H. Charap, *J. Appl. Phys.* **43**, 4190 (1972).
- <sup>28</sup>K. Nishioka, C. Hou, H. Fujiwara, and R. D. Metzger, *J. Appl. Phys.* **80**, 4528 (1996).
- <sup>29</sup>P. A. A. van der Heijden, T. F. M. M. Mass, W. J. M. de Jonge, J. C. S. Kools, F. Roozeboom, and P. J. van der Zaag, *Appl. Phys. Lett.* **72**, 492 (1998).
- <sup>30</sup>C. L. Lin, J. M. Sivertsen, and J. H. Judy, *IEEE Trans. Magn.* **31**, 4091 (1995).
- <sup>31</sup>R. P. Michel, A. Chaiken, Y. K. Kim, and L. E. Johnson, *IEEE Trans. Magn.* **32**, 4651 (1996).
- <sup>32</sup>M. T. Hutchings, B. D. Rainford, and H. J. Guggenheim, *J. Phys. C* **3**, 307 (1970); M. T. Hutchings and E. J. Samuelsen, *Phys. Rev. B* **6**, 3447 (1972).
- <sup>33</sup>K. Kurosawa, M. Miura, and S. Saito, *J. Phys. C* **13**, 1521 (1980).
- <sup>34</sup>Y. Ijiri, J. A. Borchers, R. W. Erwin, S.-H. Lee, P. J. van der Zaag, and R. M. Wolf, *Phys. Rev. Lett.* **80**, 608 (1998).
- <sup>35</sup>W. L. Roth, *Phys. Rev.* **110**, 1333 (1958); D. Hermann-Ronzaud, P. Burlet, and J. Rossat-Mingod, *J. Phys. C* **11**, 2123 (1978).
- <sup>36</sup>A. Z. Menshikov, V. A. Kazantsev, N. N. Kuzmin, and S. K. Sidorov, *J. Magn. Magn. Mater.* **1**, 91 (1975).
- <sup>37</sup>T. J. Moran, J. Nogués, D. Lederman, and I. K. Schuller, *Appl. Phys. Lett.* **72**, 617 (1998).
- <sup>38</sup>S. S. P. Parkin, V. R. Deline, R. O. Hilleke, and G. P. Felcher, *Phys. Rev. B* **42**, 10 583 (1990).